Journal of Nuclear Medicine, published on August 17, 2017 as doi:10.2967/jnumed.116.186361

CURRENT CONCEPTS IN ^{68}Ga-DOTATATE NEN IMAGING: INTERPRETATION, BIODISTRIBUTION, DOSIMETRY AND MOLECULAR STRATEGIES.

Lisa Bodei[1], Valentina Ambrosini[2], Ken Herrmann[3,4] and Irvin Modlin[5]

[1]Molecular Imaging and Therapy Service, Department of Radiology, Memorial Sloan Kettering Cancer Center, New York, USA;
[2]Nuclear Medicine, Department of Experimental Diagnostic and Specialized Medicine, University of Bologna and S. Orsola-Malpighi Hospital, Bologna, Italy;
[3]Department of Molecular and Medical Pharmacology, David Geffen School of Medicine at UCLA, USA
[4]Klinik für Nuklearmedizin, Universitätsklinikum Essen, Essen, Germany;
[5]Yale University School of Medicine, Department of Surgery, New Haven, USA.

Corresponding Author:

Lisa Bodei, MD, PhD
Molecular Imaging and Therapy Service
Department of Radiology
Memorial Sloan Kettering Cancer Center
1275 York Avenue, Box 77, New York, NY 10065
T:212.639.5387 F:212.717.5282
E:bodeil@mskcc.org

Running title: Current Concepts in ^{68}Ga-DOTATATE PET/CT

Word count: 6702

ABSTRACT

^{68}Ga-DOTATATE PET/CT provides information of the location(s) of somatostatin receptor expressing tumors. Integrating this imaging data effectively in patient care requires the clinical history, the histopathology and biomarker information as well as grade, stage and prior imaging. Previous therapies and technical aspects of the study should be considered, given their ability to alter the interpretation of the images. This includes physiologic biodistribution of the radiotracer, as well as conditions that engender false positive results.

This CME document provides a guide to the performance and interpretation of ^{68}Ga-DOTATATE PET/CT and describes its role in the diagnostic algorithm of neuroendocrine neoplasms (NEN) and is overall utility in their management.

INTRODUCTION

Neuroendocrine neoplasms exhibit variable symptomatology, such as tumor mass effects or the biological consequences of the bioactive amine secretion, frequently delaying diagnosis. Some patients present with symptoms related to inappropriate peptide or amine hypersecretion, but the majority of these tumors are nonfunctioning. Nonfunctioning tumors are usually discovered when they are large, and have metastasized to the liver. Thus, even though the lesions are mostly well-differentiated and slow-growing, with a minority of aggressive forms, the outcome may be poor due to diagnostic delay (*1*).

Somatostatin receptor imaging offers an opportunity to identify receptor expressing NENs(*2*) (*3*).

Radiolabeled somatostatin analogs (SSA) were introduced in the 1980s for imaging of NENs (*4,5*)(**Figure 1**).

CLINICAL SCENARIO OF NENs

NENs are relatively rare tumors originating from ubiquitous neuroendocrine cells distributed throughout the body. These cells synthesize, store, and secrete various circulating hormones and neurotransmitters (**Table 1**) (*6*).

NENs constitute 0.66% of all malignancies in the United States, according to the Surveillance, Epidemiology, and End Results (known as SEER) database, containing 48.195 NENs (1970-2006), with an incidence increasing at a rate of 3-10% per year (*7*). This increment is related to the introduction of more sensitive diagnostic tools, and to an increased awareness by clinicians and pathologists (*1,8*). The prevalence of NENs is substantial given the often indolent nature of the disease process. The majority (66%) arise in the the gastro-entero-pancreatic area, while 25%

occur in the lung (*7*). The recognition that the prevalence as a gastrointestinal cancer is only exceeded by that of colon cancer has increased focus on the problem (*1*).

Less frequent forms of NENs include pheochromocytoma, paraganglioma, medullary thyroid carcinoma, and neuroblastoma. Pheochromocytoma and paragangliomas derive from sympathetic chromaffin tissue in the adrenal medulla and from the extra-adrenal paraganglial system of the thorax and abdomen (*9*). The frequent malignant propensity of these tumors reflects the genetic background. Over 50% of tumors are due to genetic alterations (*10*). Pheochromocytoma exhibits an overall incidence of 0.8 cases/100,000/year over 30 years in the white population, according to the Rochester Epidemiology Project (*11*).

CLASSIFICATION

Since 1963, many NEN classifications have been adopted, based on the embryologic origin of the tumor (foregut, midgut, hindgut), degree of differentiation, and site of origin (*12*) The term "carcinoid" has been abandoned for gastro-entero-pancreatic NENs. The prognostic assessment of gastroenteropancreatic NENs has improved significantly since the introduction of the European Neuroendocrine Tumor Society (known as ENETS) and World Health Organization (WHO) 2010 staging and grading systems. The World Health Organization 2010 classification scores gastro-entero-pancreatic NENs into G1, G2 and G3, based on the morphology and Ki-67 scoring index[1] and MANEC (mixed adenoneuroendocrine carcinoma) (*13*). Although most NENs are well differentiated (G1, G2), around 5.6-8% are G3 (Ki-67>20%) (*14*). Recent evidence highlights the need to further stratify patients in the G3 group based on their different clinical behavior and response to treatment into well-differentiated NET G3 (Ki-67 20-50%) and poorly-differentiated NEC G3 (Ki-67>50%).

[1] Gastro-entero-pancreatic neuroendocrine tumor G1: Ki-67<2%; neuroendocrine tumor G2: Ki-67=3-20%; neuroendocrine carcinoma G3: Ki-67>20%

Current classification of bronchopulmonary NENs includes typical and atypical carcinoid, large cells neuroendocrine carcinoma, small-cell carcinoma and diffuse idiopathic pulmonary neuroendocrine cells hyperplasia (the latter considered a pre-invasive form). A new classification of lung neuroendocrine tumors has been proposed by the World Health Organization (*15*) and was endorsed by European Neuroendocrine Tumor Society. Similarly to gastro-entero-pancreatic NENs, this three-tier grading system is centered on Ki-67 index, with specifically generated cut-offs[2].

The tumor grading, histopathology type, primary site and staging reflect on the potential metastatic spread and, therefore, impact on the tumor burden and the subsequent choice of therapeutic options (**Table 2**). These characteristics, together with prior treatment history are fundamental when reading a ^{68}Ga-DOTATATE scan.

^{68}Ga-DOTATATE PET/CT

Indications

^{68}Ga-DOTATATE (^{68}Ga-DOTA-Tyr^{3}-Thr^{8}-octreotide) is a radiolabeled somatostatin analogue indicated for use with positron emission tomography (PET/CT) for localization of somatostatin receptor (SSR) positive NENs in adult and pediatric patients (*16*).

SSR imaging is used for staging and restaging and to select patients for therapy with “cold” or radiolabeled (PRRT) somatostatin analogs (*17,18*). The rationale of SSR imaging is the tumor cell receptor-mediated internalization of the receptor-radio-analog complex and its retention in the cytoplasm.

[2] Bronchopulmonary neuroendocrine neoplasm G1: Ki-67<4%, no necrosis; G2: Ki-67=4-25% and necrosis in <10 high-power fields (HPF); G3: Ki-67>25% and necrosis in >10 HPF.

Three SSA Peptides and Choice of DOTATATE

^{111}In-pentetreotide or OctreoScan® was the first approved radiopharmaceutical for NEN imaging. Over the past 15 years, this tracer demonstrated the utility of somatostatin receptor imaging. The development of Gallium-68-labeled agents, suitable for use with PET/CT has markedly enhanced lesion detection (due to improved resolution) and quantitation with the ^{68}Ga-labeled octreotide derivatives (^{68}Ga-SSA-PET/CT), DOTATOC (DOTA-Tyr^3-octreotide), DOTANOC (DOTA-Nal^3-octreotide), and DOTATATE (*18-20*). These analogs retain an octreotide-like affinity profile and, in particular, high affinity for SSTR2 (e.g. 0.2±0.04 nM for SSTR2 with ^{68}Ga-DOTATATE, much greater than 22±3.6 nM of ^{111}In-pentetreotide(*21*)). Only DOTANOC exhibits substantial affinity for SSTR3 (*22*). Despite these differences in receptor affinity, a clear superiority of one compound over the others has not been demonstrated. A comparison of ^{68}Ga-DOTATOC versus ^{68}Ga-DOTATATE PET/CT in the same patients, yielded comparable diagnostic accuracy, despite potential advantages for ^{68}Ga-DOTATOC in the number of detected lesions and the higher SUVmax (*23*). However, a recent comparison of ^{68}Ga-DOTATATE and ^{68}Ga-DOTANOC PET/CT in the same NEN patients, showed higher SUVmax values for ^{68}Ga-DOTATATE on a lesion basis, and comparable diagnostic accuracy on a patient basis (*24*). The inconclusive results on this issue reported in the literature possibly reflect the particular receptor configuration of the individual tumors and the lack of internationally recognized criteria for SSR PET interpretation.

Based on the demonstrated superiority of DOTATATE PET/CT imaging compared to ^{111}In-octreotide, the US Food and Drug Administration has approved ^{68}Ga-DOTATATE for localization of somatostatin receptor positive NETs in adult and pediatric patients.

Technique

The potential benefits of withdrawal of SSA treatment, or at least of scanning patients at the end of the coverage period of the analog, is still under debate and no international consensus has been reached. If discontinuation is clinically feasible and performed, short-acting analogs should be stopped for at least 48 hrs, while long-acting formulations should be discontinued for 4-6 weeks (*16*). Recent data investigating the impact of SSA on ^{68}Ga-DOTATATE PET/CT in the same patients studied on and off treatment in two consecutive days, do not support the need for discontinuation. The authors reported reduced uptake at physiologic sites with unchanged tumor uptake, in the patients under treatment, resulting in higher image contrast (*25*). Since normal organ and tumor uptake tends to increase the longer the PET scan occurs after somatostatin analogue administration (*26*) and since rigorous data on timing is unavailable, many centers scan patients at the end of the SSA treatment cycle, if possible (e.g. prior to the subsequent SSA injection), otherwise maintaining the same time interval from the SSA injection as in the previous scan.

According to the recent European Association of Nuclear Medicine guidelines and the US Food and Drug Administration approved label, the recommended activity to obtain good image quality is 2 MBq/kg of body weight (0.054 mCi/kg) up to 200 MBq (5.4 mCi) administered as intravenous bolus injection.

^{68}Ga-DOTATATE can be either supplied already labeled or as a kit to be reconstituted according to the manufacturer's (Advanced Accelerator Applications) instructions (http://www.accessdata.fda.gov/drugsatfda_docs/label/2016/208547s000lbl.pdf).

Before injection, the radioactivity should be verified with a dose calibrator. Injected radioactivity should be within ±10% of the recommended dosage.

Patients should be encouraged to drink a sufficient amount of water before administration (e.g. 1 liter, if tolerated, with or without oral contrast), following tracer administration, to increase image quality in the abdomen, and to void frequently.

The PET/CT acquisition typically begins 45-60 minutes after the intravenous administration of the radiopeptide, from top of the skull to mid thighs, preferably in a 3D mode. For a detailed description of the scanning protocol and image reconstruction, refer to the European Association of Nuclear Medicine procedure guidelines for ^{68}Ga-DOTA-peptides (*16,27*). The use of intravenous contrast media may further enhance the detection. However, in standard usage, unenhanced PET/CT is considered sufficient.

Biodistribution

The clearance of ^{68}Ga-DOTATATE from the blood is rapid. Dynamic PET studies demonstrated that arterial activity elimination is bi-exponential with no radioactive metabolites detected in serum and urine in the first 4 hrs. Radioactivity in the blood decreases to less than 5.3% of the peak level within 45 min of the dynamic scanning and to 2.2% at 195 min after injection. After 50 min, the accumulation in all organs plateaus and maximal tumor activity accumulation is reached at 70±20 min post-injection (*28*). Excretion occurs almost exclusively via the kidneys.

Physiological uptake is high in SSTR2-rich organs such as pituitary gland, spleen, adrenals, liver, pelvi-calyceal system of the kidneys and urinary bladder. Lower uptake may physiologically be observed in the thyroid, pancreatic head, stomach, small and large bowel, and prostate (**Figure 2**) (*29*).

SUV has been demonstrated to correlate with receptor density up to values of approximately 25, corresponding to the steady-state Ki values of 0.2 mL/cm3/min, after which the relationship is not linear, and this may lead to underestimation of receptor expression (*28*).

Dosimetry

Estimated absorbed doses per injected activity for organs and tissues follow the biodistribution, peaking at 1, 2, and 3 h post-injection in the spleen, followed by kidneys and liver (**Table 3**). The highest absorbed doses are observed in the spleen and urinary bladder wall, followed by kidney, adrenals, and liver. The reported total effective dose was 0.021±0.003 mSv/MBq (*30*).

The effective radiation dose resulting from the administration of 185 MBq (5 mCi) to an adult weighing 75 kg, is about 4.8 mSv (*31*). For this activity, the typical radiation dose to the critical organs, which are the urinary bladder wall, the spleen, and the kidneys, are about 0.125, 0.282, and 0.0921 mSv/MBq, respectively (*31*). Since the spleen has the highest physiological uptake, higher uptake and dose to normal or tumor tissues may occur in patients with splenectomy, as demonstrated for ^{68}Ga-DOTATOC (*32*). The effective dose deriving from the low-dose CT component is generally in the range of 9 mSv for 80 mA low-dose CT, while for 10mA ultra-low dose CT it is closer to 1 mSv.

Interpretation

Assessment of images should be guided by clinical information. As a general rule, besides areas of physiologic uptake, clearly outlined foci of uptake should be regarded as positive for SSR expression and thus considered to potentially represent neuroendocrine neoplasm (**Figure 3**,

Supplemental Figure 1). ^{68}Ga-DOTATATE has certain limitations which have to be taken into account to adequately interpret the corresponding scans. There are alternative conditions that may exhibit increased SSR expression and hence, represent potential sources of false positives (**Figure 4**, **5**, **Supplemental Figure 2**). These mainly include areas of inflammation or infection containing activated lymphocytes and macrophages, such as radiation pneumonitis, gastritis, sequelae of recent surgeries, reactive lymphadenopathy and granulomatous lesions. For example, the thyroid generally exhibits low-grade uptake (SUVmax 1.4-7.7, SUVmean 3.0(*29*)). More intense diffuse uptake could represent thyroiditis (due to the SSR-positive diffuse lymphocyte infiltration), while focal uptake could represent nodular disease (*33*). An area that requires careful consideration is the head of the pancreas, particularly the uncinate process, which may exhibit a variable physiologic uptake, focal or diffuse, of ^{68}Ga-DOTATATE, related to the great concentration of pancreatic polypeptide cells (*16*). This represents a potential source of misinterpretation, since the pancreas and the duodenum are frequent sites of NENs. There have been attempts at defining a SUVmax threshold to distinguish benign from malignant pancreatic uptake of DOTA-SSA peptides (*34,35*). However, given the large overlap between benign/physiologic and malignant uptake and the large inter-scanner measurement variance, the mere uptake should not be used to diagnose pancreatic NENs without the demonstration of a clear lesion at the companion CT or at correlative diagnostic cross-sectional imaging (*36*). Other common non NEN-related sources of uptake include accessory spleens/splenules, which could be erroneously interpreted as lymph nodes. If sufficiently large, consideration of lesion attenuation and arterial-phase contrast behavior may be of assistance (**Figure 6**).

Prolonged therapy with “cold” SSA may reduce the background physiologic uptake to the spleen and liver.

False negatives are most commonly related to lesion size (spatial resolution is around 5.5-7 mm with potential additional detrimental effects due to partial volume effect, **Figure 7**), recent analog therapy (although this issue is debated), alteration of receptor expression by recent chemotherapy or truly receptor-negative disease (e.g. benign insulinomas, high grade NENs). In case of high-grade tumors, correlation with FDG PET/CT may be useful. High physiological uptake as previously described in organs such as spleen, liver, adrenals, pituitary gland, in the pelvi-calyceal system of the kidneys and urinary bladder, and to a lesser degree in the thyroid, pancreatic head, stomach, small and large bowel, and prostate can mask iso-intense or small pathological SSTR2 expression.

Clinical Value

^{68}Ga-DOTA-peptides PET/CT is the gold standard functional imaging modality to study well differentiated NENs in Europe and is included in European guidelines (*16*). In the past decade, many reports demonstrated the superiority of SSR PET/CT (with DOTATATE, DOTATOC or DOTANOC) over single photon scintigraphy (including SPECT/CT), morphological imaging (CT/MR) or PET/CT with other radiopharmaceuticals (*16,19,20,37-41*). In a recent prospective trial including 131 patients with gastroenteropancreatic NENs and unknown primary NENs, ^{68}Ga-DOTATATE showed a higher detection rate (95.2%) compared to ^{111}In-pentetreotide SPECT/CT (30.9%) and CT or MRI (45.6%) (*42*).

The largest single study specifically addressing ^{68}Ga-DOTATATE diagnostic accuracy in NENs (*39*) was retrospective and included 728 patients and 1,258 PET/CT scans. ^{68}Ga-DOTATATE PET/CT showed high sensitivity (>94%) and specificity (>92%) for NEN lesion localization, with the highest accuracy for primary midgut tumors. The results reported by

Skoura et al. are in line with the ones reported in much smaller previous studies using PET/CT with either DOTATOC or DOTANOC (*16,20,43-46*). Overall, somatostatin receptor PET/CT showed a high accuracy (≥96%) for the detection of well-differentiated NENs at either the primary or the metastatic sites (mostly lymph nodes, liver, bone, lung) (*20,39,44*).

Current guidelines indicate the high diagnostic accuracy of somatostatin receptor PET/CT for detecting disease extension (at both staging and restaging), identification of the unknown primary site and selection of candidates for PRRT (*16*).

The role of PET/CT for the assessment of tumor response to treatment is still under debate since a reduction of uptake can indicate a reduction of tumor volume (and of receptor number) but cannot exclude the presence of undifferentiated clones that may be SSR-negative. Considering the fact that SSR PET/CT positivity predicts the localization of "cold" and radiolabeled SSA-based treatment options, it is evident that the clinical impact of ^{68}Ga-DOTATATE relies not merely in a better diagnostic accuracy but also impacts therapeutic management with cold SSA or PRRT.

A recently published systematic review (*47*) (including data from 1,561 patients) reported an overall change in management in 44% (range: 16-71%) after ^{68}Ga-SSA-PET/CT (with either DOTATOC, DOTATATE or DOTANOC). About half of these cases were provided by a single study employing ^{68}Ga-DOTATATE (728/1561, 47%) (*39*). Skoura et al. reported that the treatment plan was changed in 40.9% (515/1278) of the ^{68}Ga-DOTATATE PET/CT because of new, unexpected findings. In most cases the new treatment comprised chemotherapy or PRRT (70.3%, 362/515) while less frequent options include surgery (after detection/confirmation of NEN primary site, 10.1%, 52/515) and second-line chemotherapy (13.8%, 71/515). Less common management changes included ongoing treatment discontinuation (2/515), rejection of PRRT (2/515), and

selection of liver transplant candidates by excluding extrahepatic disease (2/515). Previous reports in smaller patient population reported similar findings (*42*).

^{68}Ga-SSA-PET/CT has also been demonstrated to provide relevant prognostic information: since the intensity of uptake is an indirect measure of tumor differentiation, higher uptake correlated with a better prognosis (*48*).

The role of ^{68}Ga-SSA-PET/CT in the G3 NENs is debated. By definition, G3 includes poorly differentiated tumors, however, especially in the subgroup with Ki-67 20-50%, the clinical behavior is more similar to G2 tumors. In this setting, a complementary role with FDG can therefore be envisioned. Vice versa, ^{68}Ga-SSA-PET/CT in cases presenting higher Ki67>50%, even if positive, will likely not impact management.

The added value of FDG in the well-differentiated NENs (G1 and G2) is still under debate and no international consensus has been reached (*49-53*).

According to current evidence, the role of FDG is not routinely recommended in G1 NENs (where it could be considered only in selected cases when a specific clinical indication/suspicion is present), while it may have a clinical role in G2 NENs, especially for higher Ki-67 values, based on clinical indications (e.g. patients with CT progression or with SR PET/CT negative lesions). Recently, it was in fact shown that ^{18}FDG-PET/CT should be only used in selected cases for Ki-67<12% (*53*) as here the clinical management uniquely relies on ^{68}Ga-DOTATATE.

Current European Neuroendocrine Tumor Society guidelines (2016) indicate a potential role for FDG only for the G3 group, when surgery is indicated. Several studies, mostly retrospective, investigated the role of combination of ^{68}Ga-SSA-PET/CT and FDG-PET/CT in NENs. However, they were hampered by small patient population and by the heterogeneity of the tumor primary site (a well-known factor affecting FDG positivity). In a recent multinational,

multidisciplinary Delphi consensus meeting of NEN experts (n = 33) (*54*), ^{18}FDG-PET/CT was considered valuable for differentiating high- from low-grade tumors, and for its prognostic implications. No consensus, however, was reached regarding combining ^{18}FDG- and ^{68}Ga-SSA-PET/CT or their timing in a diagnostic setting.

A combined imaging modality to achieve a complete biological characterization defining a more aggressive behavior is appealing. In fact, the mere detection of a higher number of lesions or even the detection of FDG-positivity is not necessarily associated to a different management in all cases and nuclear medicine/oncology departments. However, there is international consensus on the fact that FDG positivity correlates with a worse prognosis (*55*), but, the treatment strategies to be implemented in FDG positive cases are not standardized. The rationale for employing FDG relies on its ability to identify the presence of aggressive disease foci that may turn into a better stratification of patients at major risk for progression. The clinical scenario of double-tracer imaging findings ranges from purely SSR-positive/FDG-negative cases to FDG-positive/SSR-negative cases, with a very heterogeneous intermediate group presenting various patterns of uptake in the same patient with both tracers in the same or in different lesions over time (*52*). The most important lesson deriving from these studies is the demonstration of the heterogeneous nature of NENs.

SSR imaging is used to select patients for PRRT. While the criteria are well-defined and validated for OctreoScan, with the 4-point Krenning scale, based on the relative tumor uptake compared to the one of normal organs (liver, kidneys and spleen, where grade 1: uptake<liver (liver excluded), grade 2: uptake= liver, grade 3: uptake>liver, and grade 4: >>kidneys and spleen) (*4*), there is no consensus on what should be considered sufficient uptake at ^{68}Ga-SSA-PET/CT. Some authors have reported SUVmax thresholds for PRRT enrollment, based on

retrospective analyses e.g. SUVmax of 17.9 and 16.4 are reported for ^{68}Ga-DOTATOC (*56,57*). However, this approach is hampered by the limited reproducibility of SUVmax values across different scanners. More frequently in clinical practice, the Krenning scale is adapted to the volumetric ^{68}Ga-SSA-PET/CT image, and lesion uptake greater than the liver is considered suitable for PRRT.

Integration within the Diagnostic Algorithm of NENs

Biomarkers are a viable adjunct to image interpretation. The secretory activity of NENs is quantifiable and facilitates their detection. Previously chromogranin A (CgA) was considered useful but rigorous assessment over the last decade has led to decreased enthusiasm in its usage, due to normal levels in ~30-40% of NENs, and falsely elevated levels in patients with renal failure, cardiac disease or PPI therapy (*58*). Moreover, alterations in circulating CgA levels are often non-concordant with imaging and prospective studies have not confirmed a role for CgA in predicting or defining progression (*54*). To better reflect, besides the mere secretory activity, the complex biological activities of an evolving neoplasm (cell proliferation, growth factor signaling, etc), that constitute the "hallmarks of cancer", and provide more relevant information on tumor behavior, new approaches have been introduced, including whole genomic sequencing, circulating miRNA and tumor transcripts (*59*). Evaluation of circulating mRNA (transcript analysis) has provided information on disease status that is of substantial clinical utility in clinical management of NENs (*60,61*). This strategy utilizes simultaneous PCR-based analyses of multiple NET genes measurable in the blood and algorhythmic transformation into a mathematical index of disease activity (*59,62*). NEN gene blood levels correlated with ^{68}Ga-DOTA-SSA PET/CT imaging and could define disease status (*63*).

Current imaging strategies and biomarkers in NEN management addressed at a recent Delphi consensus meeting of NEN experts (*54*), indicated agreement on the use of CT or MRI in conjunction with functional imaging. Due to its synergistic value ^{68}Ga-DOTATATE is often used in addition to morphological imaging modalities such as CT and MRI. PET/CT scanners are widely available and the corresponding CT, if performed with diagnostic quality and contrast media, may improve the diagnostic accuracy particularly in organs with high physiologic ^{68}Ga-DOTATATE uptake and in the lung. Especially gastroenteropancreatic NENs are well suited for dedicated PET/MRI as MRI adds important information to the detection of abdominal lesions, particularly in the liver (**Supplemental Figure 3**) (*64,65*) whereas CT remains superior for the detection and characterization of lung lesions. As discussed, ^{18}FDG detects dedifferentiated lesions expressing no or few SSTR2 (*53*). A common indication for ^{18}FDG-PET/CT is morphologically growing lesions with a discordant ^{68}Ga-DOTATATE finding.

These observations are worthy of further clinical study to provide evidence that the interface of imaging and circulating molecular indices of tumor evolution is likely to enhance dynamic assessment of tumor status.

^{68}Ga-DOTA-peptides PET/CT has significantly advanced the approach to NENs. Its widespread implementation is based upon its proven clinical utility and facilitation of clinical management. Overall it represents the gold standard functional imaging modality for the assessment of well-differentiated NENs in conjunction with anatomic imaging (CT/MR). An unmet need is the evaluation of the clinical impact of the dual approach ^{18}F-FDG- and ^{68}Ga-SSA-PET/CT in the decision-making algorithm, given the numerous indications from literature of the prognostic impact of FDG avidity in terms of overall and treatment-specific survival. A further

significant advance needed is the development of an accurate, personalized interpretation of the individual disease status.

This may be accomplished by the development of an algorithmic integration of information obtained from synthesis of the clinical, histopathological, imaging and molecular information available from the neoplasm of each subject.

DISCLOSURE

LB is a consultant for AAA and Ipsen, KH is a consultant for Sofie Biosciences. No other potential conflict of interest relevant to this article was reported.

REFERENCES

1. Modlin IM, Oberg K, Chung DC, et al. Gastroenteropancreatic neuroendocrine tumours. *Lancet Oncol.* 2008;9:61-72.

2. Sundin A. Radiological and nuclear medicine imaging of gastroenteropancreatic neuroendocrine tumours. *Best Pract Res Clin Gastroenterol.* 2012;26:803-818.

3. Oberg K. Diagnostic work-up of gastroenteropancreatic neuroendocrine tumors. *Clinics (Sao Paulo).* 2012;67 Suppl 1:109-112.

4. Kwekkeboom DJ, Kam BL, van Essen M, et al. Somatostatin-receptor-based imaging and therapy of gastroenteropancreatic neuroendocrine tumors. *Endocr Relat Cancer.* 2010;17:R53-73.

5. Crona J, Skogseid B. GEP- NETS UPDATE: Genetics of neuroendocrine tumors. *Eur J Endocrinol.* 2016;174:R275-290.

6. Polak JM, Bloom SR. Regulatory peptides of the gastrointestinal and respiratory tracts. *Arch Int Pharmacodyn Ther.* 1986;280:16-49.

7. Gustafsson BI, Kidd M, Modlin IM. Neuroendocrine tumors of the diffuse neuroendocrine system. *Curr Opin Oncol.* 2008;20:1-12.

8. Modlin IM, Champaneria MC, Chan AK, Kidd M. A three-decade analysis of 3,911 small intestinal neuroendocrine tumors: the rapid pace of no progress. *Am J Gastroenterol.* 2007;102:1464-1473.

9. Tumours of the adrenal gland - WHO and TNM classifications In: DeLellis R., Lloyd R., Heitz P., C. E, eds. *Pathology and Genetics of Tumours of the Endocrine Organs. World Health Organization Classification of Tumours Pathology and Genetics of Tumours of Endocrine Organs*. Lyon: IARC press; 2004.

10. Favier J, Amar L, Gimenez-Roqueplo AP. Paraganglioma and phaeochromocytoma: from genetics to personalized medicine. *Nat Rev Endocrinol.* 2015;11:101-111.

11. Beard CM, Sheps SG, Kurland LT, Carney JA, Lie JT. Occurrence of pheochromocytoma in Rochester, Minnesota, 1950 through 1979. *Mayo Clin Proc.* 1983;58:802-804.

12. Williams ED, Sandler M. The classification of carcinoid tum ours. *Lancet.* 1963;1:238-239.

13. Rindi G, Arnold R, al. CCe. Nomenclature and classification of digestive neuroendocrine tumours. In: Bosman F, Carneiro F, eds. *World Health Organization Classification of Tumours, Pathology and Genetics of Tumours of the Digestive System*. Lyon: IARC Press; 2010.

14. Velayoudom-Cephise FL, Duvillard P, Foucan L, et al. Are G3 ENETS neuroendocrine neoplasms heterogeneous? *Endocr Relat Cancer.* 2013;20:649-657.

15. Travis WD, Brambilla E, Nicholson AG, et al. The 2015 World Health Organization Classification of Lung Tumors: Impact of Genetic, Clinical and Radiologic Advances Since the 2004 Classification. *J Thorac Oncol.* 2015;10:1243-1260.

16. Virgolini I, Ambrosini V, Bomanji JB, et al. Procedure guidelines for PET/CT tumour imaging with 68Ga-DOTA-conjugated peptides: 68Ga-DOTA-TOC, 68Ga-DOTA-NOC, 68Ga-DOTA-TATE. *Eur J Nucl Med Mol Imaging.* 2010;37:2004-2010.

17. Bodei L, Sundin A, Kidd M, Prasad V, Modlin IM. The status of neuroendocrine tumor imaging: from darkness to light? *Neuroendocrinology.* 2015;101:1-17.

18. Ambrosini V, Morigi JJ, Nanni C, Castellucci P, Fanti S. Current status of PET imaging of neuroendocrine tumours ([18F]FDOPA, [68Ga]tracers, [11C]/[18F]-HTP). *Q J Nucl Med Mol Imaging.* 2015;59:58-69.

19. Treglia G, Castaldi P, Rindi G, Giordano A, Rufini V. Diagnostic performance of Gallium-68 somatostatin receptor PET and PET/CT in patients with thoracic and gastroenteropancreatic neuroendocrine tumours: a meta-analysis. *Endocrine.* 2012;42:80-87.

20. Gabriel M, Decristoforo C, Kendler D, et al. 68Ga-DOTA-Tyr3-octreotide PET in neuroendocrine tumors: comparison with somatostatin receptor scintigraphy and CT. *J Nucl Med.* 2007;48:508-518.

21. Reubi JC, Schar JC, Waser B, et al. Affinity profiles for human somatostatin receptor subtypes SST1-SST5 of somatostatin radiotracers selected for scintigraphic and radiotherapeutic use. *Eur J Nucl Med.* 2000;27:273-282.

22. Reubi JC, Waser B, Schaer JC, Laissue JA. Somatostatin receptor sst1-sst5 expression in normal and neoplastic human tissues using receptor autoradiography with subtype-selective ligands. *Eur J Nucl Med.* 2001;28:836-846.

23. Poeppel TD, Binse I, Petersenn S, et al. 68Ga-DOTATOC versus 68Ga-DOTATATE PET/CT in functional imaging of neuroendocrine tumors. *J Nucl Med.* 2011;52:1864-1870.

24. Kabasakal L, Demirci E, Ocak M, et al. Comparison of (6)(8)Ga-DOTATATE and (6)(8)Ga-DOTANOC PET/CT imaging in the same patient group with neuroendocrine tumours. *Eur J Nucl Med Mol Imaging.* 2012;39:1271-1277.

25. Interim Results on the Influence of Lanreotide on Uptake of [68Ga]-DOTATATE in Patients With Metastatic or Unresectable NET: No Evidence for Discontinuation of Lanreotide Before [68Ga]-DOTATATE PET/CT. *Clin Adv Hematol Oncol.* 2016;14:13-15.

26. Haug AR, Rominger A, Mustafa M, et al. Treatment with octreotide does not reduce tumor uptake of (68)Ga-DOTATATE as measured by PET/CT in patients with neuroendocrine tumors. *J Nucl Med.* 2011;52:1679-1683.

27. Bozkurt MF, Virgolini I, Balogova S, et al. Guideline for PET/CT imaging of neuroendocrine neoplasms with 68Ga-DOTA-conjugated somatostatin receptor targeting peptides and 18F-DOPA. *Eur J Nucl Med Mol Imaging.* 2017.

28. Velikyan I, Sundin A, Sorensen J, et al. Quantitative and qualitative intrapatient comparison of 68Ga-DOTATOC and 68Ga-DOTATATE: net uptake rate for accurate quantification. *J Nucl Med.* 2014;55:204-210.

29. Shastry M, Kayani I, Wild D, et al. Distribution pattern of 68Ga-DOTATATE in disease-free patients. *Nucl Med Commun.* 2010;31:1025-1032.

30. Sandstrom M, Velikyan I, Garske-Roman U, et al. Comparative biodistribution and radiation dosimetry of 68Ga-DOTATOC and 68Ga-DOTATATE in patients with neuroendocrine tumors. *J Nucl Med.* 2013;54:1755-1759.

31. Walker RC, Smith GT, Liu E, Moore B, Clanton J, Stabin M. Measured human dosimetry of 68Ga-DOTATATE. *J Nucl Med.* 2013;54:855-860.

32. Kratochwil C, Mavriopoulou E, Rath D, et al. Comparison of 68Ga-DOTATOC biodistribution in patients with and without spleenectomy. *Q J Nucl Med Mol Imaging.* 2015;59:116-120.

33. Lincke T, Singer J, Kluge R, Sabri O, Paschke R. Relative quantification of indium-111 pentetreotide and gallium-68 DOTATOC uptake in the thyroid gland and association with thyroid pathologies. *Thyroid.* 2009;19:381-389.

34. Prasad V, Baum RP. Biodistribution of the Ga-68 labeled somatostatin analogue DOTA-NOC in patients with neuroendocrine tumors: characterization of uptake in normal organs and tumor lesions. *Q J Nucl Med Mol Imaging.* 2010;54:61-67.

35. Kroiss A, Putzer D, Decristoforo C, et al. 68Ga-DOTA-TOC uptake in neuroendocrine tumour and healthy tissue: differentiation of physiological uptake and pathological processes in PET/CT. *Eur J Nucl Med Mol Imaging.* 2013;40:514-523.

36. Virgolini I, Gabriel M, Kroiss A, et al. Current knowledge on the sensitivity of the (68)Ga-somatostatin receptor positron emission tomography and the SUVmax reference range for management of pancreatic neuroendocrine tumours. *Eur J Nucl Med Mol Imaging.* 2016;43:2072-2083.

37. Ambrosini V, Tomassetti P, Castellucci P, et al. Comparison between 68Ga-DOTA-NOC and 18F-DOPA PET for the detection of gastro-entero-pancreatic and lung neuro-endocrine tumours. *Eur J Nucl Med Mol Imaging.* 2008;35:1431-1438.

38. Srirajaskanthan R, Kayani I, Quigley AM, Soh J, Caplin ME, Bomanji J. The role of 68Ga-DOTATATE PET in patients with neuroendocrine tumors and negative or equivocal findings on 111In-DTPA-octreotide scintigraphy. *J Nucl Med.* 2010;51:875-882.

39. Skoura E, Michopoulou S, Mohmaduvesh M, et al. The Impact of 68Ga-DOTATATE PET/CT Imaging on Management of Patients with Neuroendocrine Tumors: Experience from a National Referral Center in the United Kingdom. *J Nucl Med.* 2016;57:34-40.

40. Deppen SA, Blume J, Bobbey AJ, et al. 68Ga-DOTATATE Compared with 111In-DTPA-Octreotide and Conventional Imaging for Pulmonary and Gastroenteropancreatic Neuroendocrine Tumors: A Systematic Review and Meta-Analysis. *J Nucl Med.* 2016;57:872-878.

41. Ambrosini V, Campana D, Tomassetti P, Fanti S. (6)(8)Ga-labelled peptides for diagnosis of gastroenteropancreatic NET. *Eur J Nucl Med Mol Imaging.* 2012;39 Suppl 1:S52-60.

42. Sadowski SM, Neychev V, Millo C, et al. Prospective Study of 68Ga-DOTATATE Positron Emission Tomography/Computed Tomography for Detecting Gastro-Entero-Pancreatic Neuroendocrine Tumors and Unknown Primary Sites. *J Clin Oncol.* 2016;34:588-596.

43. Putzer D, Gabriel M, Henninger B, et al. Bone metastases in patients with neuroendocrine tumor: 68Ga-DOTA-Tyr3-octreotide PET in comparison to CT and bone scintigraphy. *J Nucl Med.* 2009;50:1214-1221.

44. Ambrosini V, Nanni C, Zompatori M, et al. (68)Ga-DOTA-NOC PET/CT in comparison with CT for the detection of bone metastasis in patients with neuroendocrine tumours. *Eur J Nucl Med Mol Imaging.* 2010;37:722-727.

45. Haug A, Auernhammer CJ, Wangler B, et al. Intraindividual comparison of 68Ga-DOTA-TATE and 18F-DOPA PET in patients with well-differentiated metastatic neuroendocrine tumours. *Eur J Nucl Med Mol Imaging.* 2009;36:765-770.

46. Kayani I, Conry BG, Groves AM, et al. A comparison of 68Ga-DOTATATE and 18F-FDG PET/CT in pulmonary neuroendocrine tumors. *J Nucl Med.* 2009;50:1927-1932.

47. Fendler WP, Barrio M, Spick C, et al. 68Ga-DOTATATE PET/CT Interobserver Agreement for Neuroendocrine Tumor Assessment: Results of a Prospective Study on 50 Patients. *J Nucl Med.* 2017;58:307-311.

48. Campana D, Ambrosini V, Pezzilli R, et al. Standardized uptake values of (68)Ga-DOTANOC PET: a promising prognostic tool in neuroendocrine tumors. *J Nucl Med.* 2010;51:353-359.

49. Partelli S, Rinzivillo M, Maurizi A, et al. The role of combined Ga-DOTANOC and (18)FDG PET/CT in the management of patients with pancreatic neuroendocrine tumors. *Neuroendocrinology.* 2014;100:293-299.

50. Kundu P, Lata S, Sharma P, Singh H, Malhotra A, Bal C. Prospective evaluation of (68)Ga-DOTANOC PET-CT in differentiated thyroid cancer patients with raised thyroglobulin and negative (131)I-whole body scan: comparison with (18)F-FDG PET-CT. *Eur J Nucl Med Mol Imaging.* 2014;41:1354-1362.

51. Bahri H, Laurence L, Edeline J, et al. High prognostic value of 18F-FDG PET for metastatic gastroenteropancreatic neuroendocrine tumors: a long-term evaluation. *J Nucl Med.* 2014;55:1786-1790.

52. Nilica B, Waitz D, Stevanovic V, et al. Direct comparison of (68)Ga-DOTA-TOC and (18)F-FDG PET/CT in the follow-up of patients with neuroendocrine tumour treated with the first full peptide receptor radionuclide therapy cycle. *Eur J Nucl Med Mol Imaging.* 2016;43:1585-1592.

53. Panagiotidis E, Alshammari A, Michopoulou S, et al. Comparison of the Impact of 68Ga-DOTATATE and 18F-FDG PET/CT on Clinical Management in Patients with Neuroendocrine Tumors. *J Nucl Med.* 2017;58:91-96.

54. Oberg K, Krenning E, Sundin A, et al. A Delphic consensus assessment: imaging and biomarkers in gastroenteropancreatic neuroendocrine tumor disease management. *Endocr Connect.* 2016;5:174-187.

55. Binderup T, Knigge U, Loft A, Federspiel B, Kjaer A. 18F-fluorodeoxyglucose positron emission tomography predicts survival of patients with neuroendocrine tumors. *Clin Cancer Res.* 2010;16:978-985.

56. Oksuz MO, Winter L, Pfannenberg C, et al. Peptide receptor radionuclide therapy of neuroendocrine tumors with (90)Y-DOTATOC: is treatment response predictable by pre-therapeutic uptake of (68)Ga-DOTATOC? *Diagn Interv Imaging.* 2014;95:289-300.

57. Kratochwil C, Stefanova M, Mavriopoulou E, et al. SUV of [68Ga]DOTATOC-PET/CT Predicts Response Probability of PRRT in Neuroendocrine Tumors. *Mol Imaging Biol.* 2015;17:313-318.

58. Jensen EH, Kvols L, McLoughlin JM, et al. Biomarkers predict outcomes following cytoreductive surgery for hepatic metastases from functional carcinoid tumors. *Ann Surg Oncol.* 2007;14:780-785.

59. Oberg K, Modlin IM, De Herder W, et al. Consensus on biomarkers for neuroendocrine tumour disease. *Lancet Oncol.* 2015;16:e435-446.

60. Pavel M, Jann H, Prasad V, Drozdov I, Modlin IM, Kidd M. NET Blood Transcript Analysis Defines the Crossing of the Clinical Rubicon: When Stable Disease Becomes Progressive. *Neuroendocrinology.* 2017;104:170-182.

61. Modlin IM, Drozdov I, Kidd M. The identification of gut neuroendocrine tumor disease by multiple synchronous transcript analysis in blood. *PLoS One.* 2013;8:e63364.

62. Modlin IM, Drozdov I, Alaimo D, et al. A multianalyte PCR blood test outperforms single analyte ELISAs (chromogranin A, pancreastatin, neurokinin A) for neuroendocrine tumor detection. *Endocr Relat Cancer.* 2014;21:615-628.

63. Bodei L, Kidd M, Modlin IM, et al. Gene transcript analysis blood values correlate with (6)(8)Ga-DOTA-somatostatin analog (SSA) PET/CT imaging in neuroendocrine tumors and can define disease status. *Eur J Nucl Med Mol Imaging.* 2015;42:1341-1352.

64. Hope TA, Pampaloni MH, Nakakura E, et al. Simultaneous (68)Ga-DOTA-TOC PET/MRI with gadoxetate disodium in patients with neuroendocrine tumor. *Abdom Imaging.* 2015;40:1432-1440.

65. Beiderwellen KJ, Poeppel TD, Hartung-Knemeyer V, et al. Simultaneous 68Ga-DOTATOC PET/MRI in patients with gastroenteropancreatic neuroendocrine tumors: initial results. *Invest Radiol.* 2013;48:273-279.

66. Herrmann K, Czernin J, Wolin EM, et al. Impact of 68Ga-DOTATATE PET/CT on the management of neuroendocrine tumors: the referring physician's perspective. *J Nucl Med.* 2015;56:70-75.

FIGURE LEGENDS

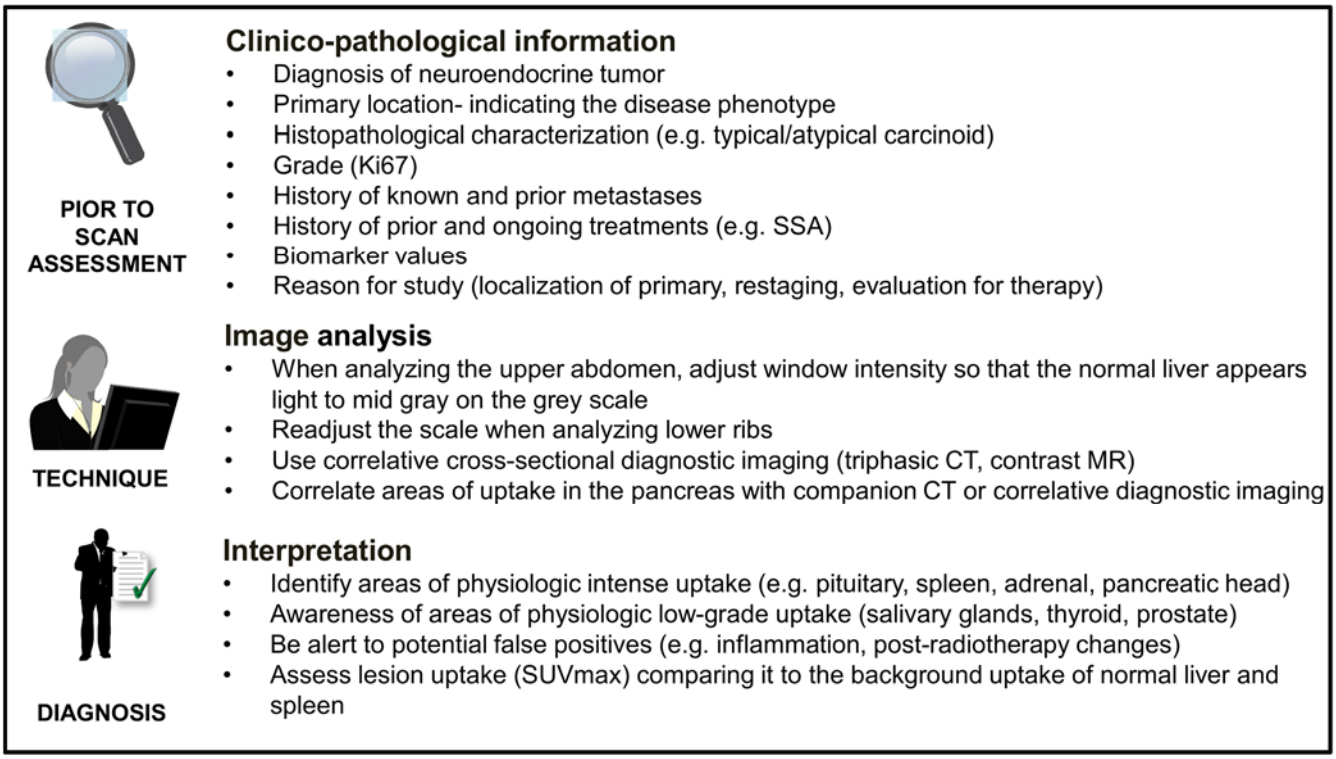

Figure 1. Optimal strategy for ^{68}Ga-DOTATATE PET/CT evaluation

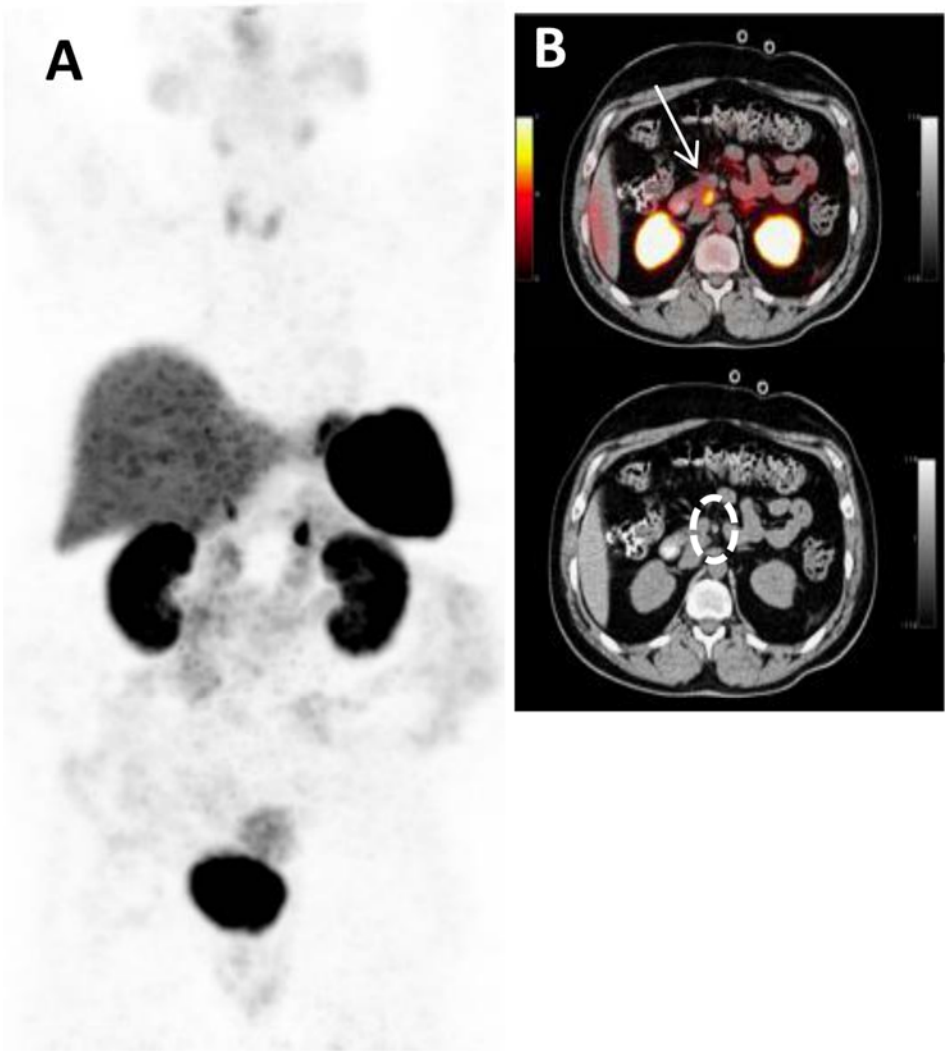

Figure 2. Normal bio-distribution of ^{68}Ga-DOTATATE (A). Physiologic intense uptake is noted in the pituitary, liver, spleen, kidneys, adrenals, and uncinate process of the pancreas (*B, solid arrow, dashed circle*) Variable degree of uptake in the thyroid, intestine, and urinary bladder.

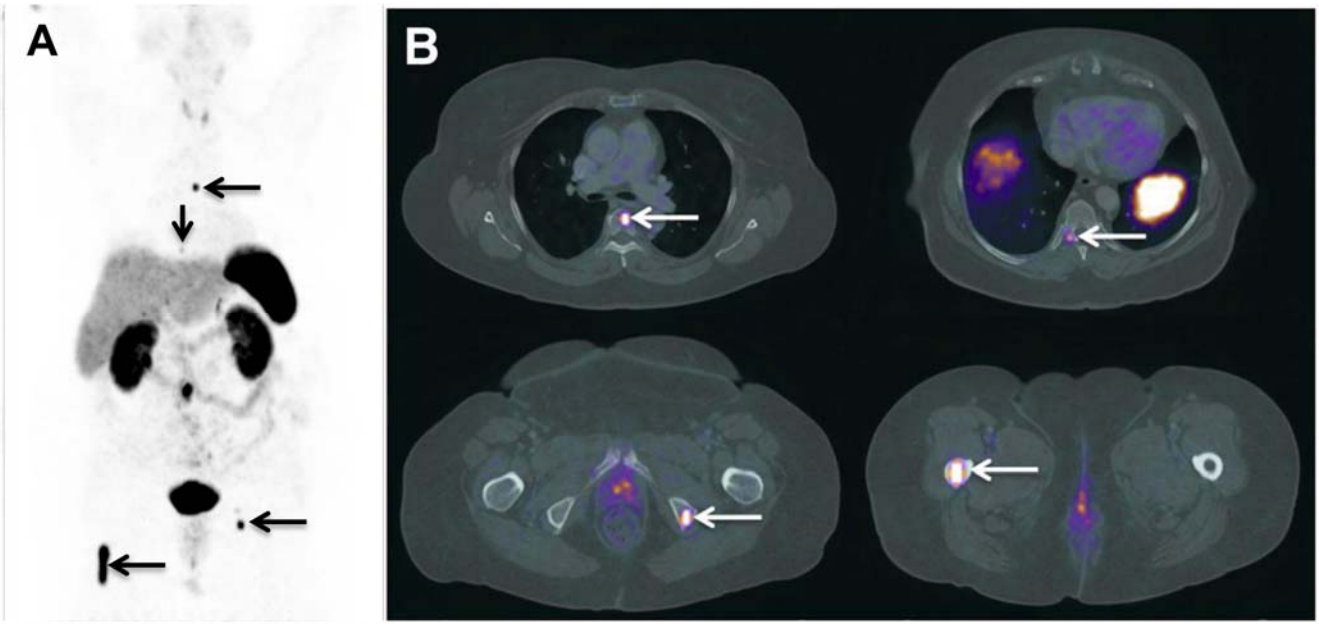

Figure 3. Upstaging of a patient with history of small-intestine NEN and a 6.5-cm lesion within the right proximal femur with benign appearance at prior MR. Unexpected soft-tissue and bone metastases were detected *(arrows,B)*. The intended treatment was converted from surgery and octreotide to surgery, octreotide, plus selective radiotherapy of bone metastases (adapted from (*66*).

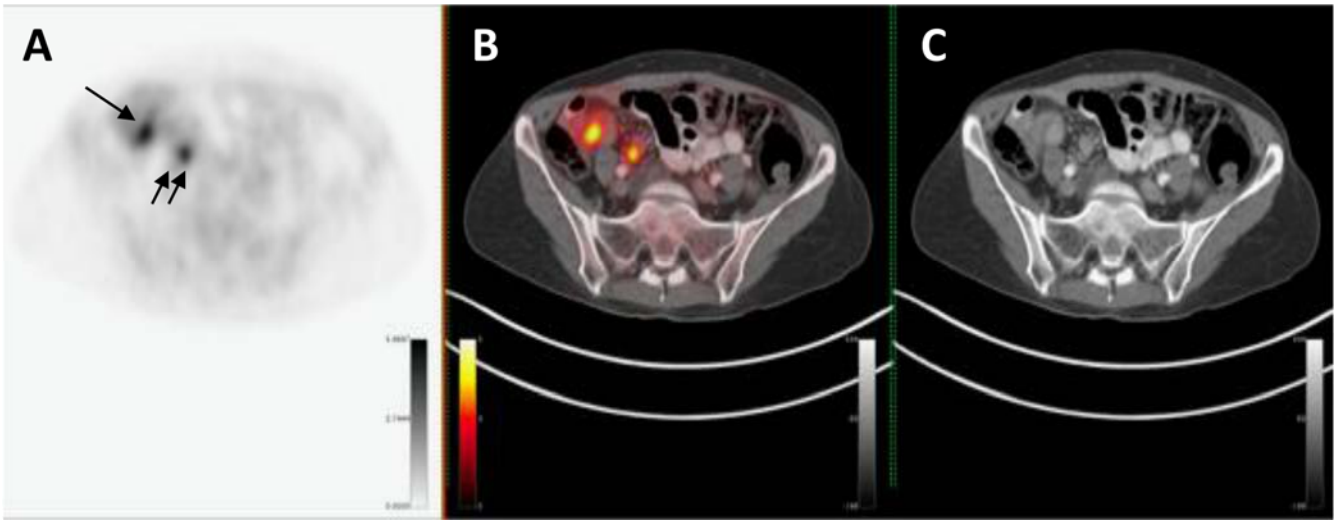

Figure 4. Patient with ileal NET (*single arrow*) presented additional focal uptake (*two arrows*) in the pelvis [*axial views of PET (A), fused PET/CT (B) and CT (C)*]. Fused PET/CT images clarified this finding as physiologic uptake in the right ureter.

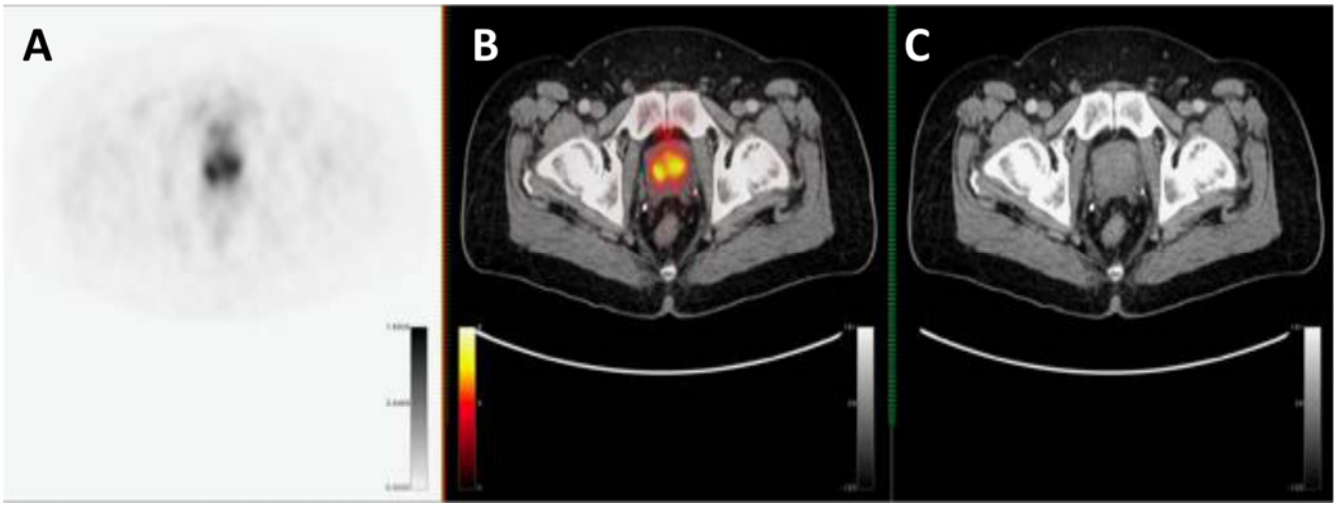

Figure 5. Increased ^{68}Ga-DOTATATE prostatatic uptake. Axial projections of PET *[(A), fused PET/CT (B) and CT (C)]*. The patient had known BPH and the corresponding uptake is therefore non-tumor specific.

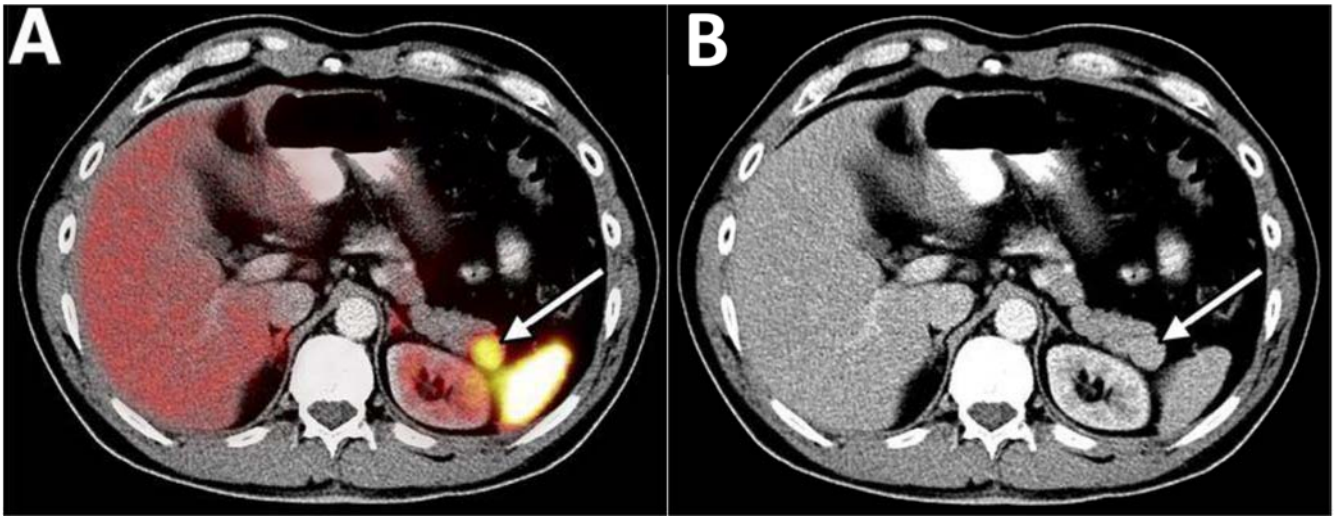

Figure 6. Patient with repeated flushing underwent ^{68}Ga-DOTATATE PET/CT [*axial fused PET/CT (A) and CT (B) images*]. Focal uptake (*arrow*) in the pancreatic tail was characterized based on clinical data and MRI, indicating the presence of a splenule abutting the tail of pancreas (reprinted from (*47*)).

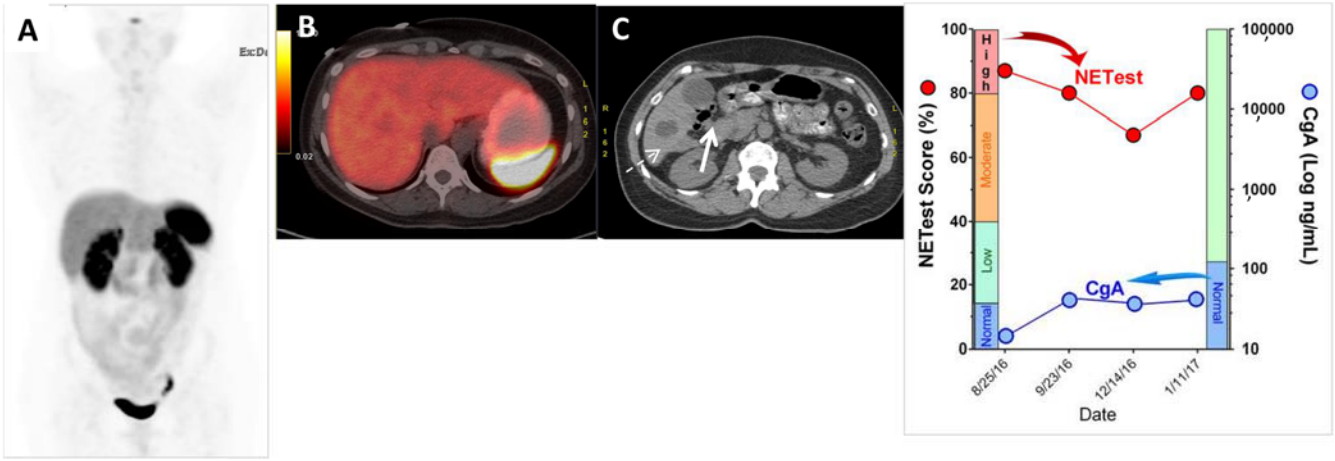

Figure 7. 60yo female previously undergone ileal NET resection, currently on SSA with associated cholelithiasis scheduled for surgery (*solid arrow,* **C**). Prior to surgery, ^{68}Ga-DOTATATE PET/CT *(***A**, **B,** simple hepatic cyst, *dashed arrow, **C**)* and CgA *(blue circles, **D**)* were negative. However, circulating neuroendocrine transcripts levels (red circles, **D**) were positive. Positive transcript levels are indicative of the presence of primary, residual or metastatic NET. At cholecystectomy, there was no evidence of hepatic metastases. Random intra-operative hepatic needle biopsy, however, demonstrated the presence of neuroendocrine tumor metastases.

Table 1. Gastrointestinal and Pancreatic Neuroendocrine Cell Types and Secretory Products

Cell type	Localization	Products
Delta (D)	Entire GI tract	Somatostatin
Enterochromaffin (EC)	Entire GI tract	Serotonin/substance P/guanylin/melatonin
Enterochromaffin-like (ECL)	Gastric fundus	Histamine
Gastrin (G)	Gastric antrum & duodenum	Gastrin
Ghrelin (Gr)	Entire GI tract	Ghrelin
I	Duodenum	CCK
K	Duodenum/jejunum	GIP
L	Small intestine	GLP-1, PYY, NPY
Motilin (M)	Duodenum	Motilin
Neurotensin (N)	Small intestine	Neurotensin
Secretin (S)	Duodenum	Secretin
Vasoactive intestinal peptide (VIP)	Entire GI tract	VIP
X	Stomach: fundus and antrum	Amylin
Beta	Pancreas	Insulin
Alpha	Pancreas	Glucagon
Delta	Pancreas	Somatostatin
Pancreatic Polypeptide (PP)	Pancreas	PP

CCK = cholecystokinin; GIP = gastric inhibitory peptide; GLP-1 = glucagon-like peptide 1; PYY = *polypeptide YY (tyrosine,tyrosine)*; NPY = neuropeptide Y (tyrosine); PP = pancreatic polypeptide.

Table 2. Characterization and Clinical Presentation of gastro-entero-pancreatic and broncho-pulmonary NENs

Site	Clinical presentation
Gastrointestinal	
Gastric	- Type I: atrophic gastritis-gastrin dependent - Type II (MEN1): Menin dependent-gastrin related (ZES) - Type III: gastrin independent; clinically aggressive
Duodenal	Various phenotypes: gastrinoma, so-called "carcinoid," somatostatinoma
Jejunal	"carcinoid"—classic symptoms (flushing, diarrhea); clinically aggressive
Ileal	"carcinoid" —classic symptoms (flushing, diarrhea); clinically aggressive. Typical CT appearance of contrast enhancing spiculated mass, sometimes containing calcifications, surrounded by lines of desmoplastic reactions.
Appendiceal	-"Carcinoid": usually present as appendicitis or incidental finding at laparotomy/laparoscopy and generally radically cured after surgical excision ; -Goblet cell carcinoid (mucinous carcinoid): clinically aggressive.
Colonic	Carcinoid symptoms are rare, presentation similar to adenocarcinoma
Rectal	Local manifestations—pain, bleeding
Hepatic	>95% are metastases from gastro-entero-pancreatic NEN primary. Typical CT appearance of hypodense masses, with rich enhancement during the arterial phase, reverting to hypodense during the portal phase. At MR (most sensitive technique) lesions enhance after gadolinium, arterial phase and fast spin-echo T2-weighted sequences are the best sequences
Pancreatic	
Gastrinoma (Zollinger-Ellison Syndrome)	Peptic ulceration and secretory diarrhea; 60-90% malignant behavior
Insulinoma	Hypoglycemia; generally small and somatostatin receptor (SSR) negative; 5–15% malignant and generally SSR-positive
Glucagonoma	Skin rash (migrating necrolytic erythema), weight loss, diabetes; 60% malignant
VIPoma	Secretory diarrhea (Verner-Morrison syndrome); 80% malignant
Somatostatinoma	Diabetes, gallstones; often a component of a genetic syndrome; 60% malignant
GRFoma	Acromegaly; 30% malignant
ACTHoma	Present as Cushing syndrome; aggressive behavior; >90% malignant
P-NEN causing carcinoid syndrome	Diarrhea, flushing; 68–88% malignant

P-NEN causing hypercalcemia	Symptoms of hypercalcemia; 80–90% malignant
Nonfunctioning	Local mass effects; 60–90% malignant.
Bronchopulmonary	
Typical carcinoid	Frequently central, with cough, wheezing, hemoptysis and signs of bronchial obstruction; functional when metastatic (carcinoid, Cushing, acromegaly or Syndrome of Inappropriate Antidiuretic Hormone Secretion, SIADH); relatively indolent biological behavior. May be part of MEN1
Atypical carcinoid	Frequently peripheral and asymptomatic; may present with coughing and wheezing or functional syndrome; from indolent to aggressive. May be part of MEN1.
Large Cell Neuroendocrine Carcinoma	Aggressively metastatic and rapidly progressing.
Small Cell Lung Cancer	Aggressively metastatic and rapidly progressing.
Thymic NETs	Frequently large, 50% functional, usually ACTH-induced Cushing syndrome. May be part of MEN1. Frequently metastatic.
Chromaffin	
Pheochromocytoma /Paraganglioma	80-85% arise from adrenal medulla, 15-20% extra-adrenal. The majority associated with catecholamine hypersecretion (most frequently, hypertension, tachycardia, headache, pallor, sweating and anxiety), with a frequent paroxysmal component

Table 3. Absorbed Doses of ^{68}Ga-DOTATATE in Selected Organs.

Anatomical Location	Absorbed dose (mGy/MBq±SD)(*30*)	Absorbed dose (mGy/MBq±SD)(*31*)
Kidney	0.093± 0.016	0.092±0.028
Liver	0.050± 0.0 15	0.045±0.015
Gallbladder wall	0.016± 0.002	0.015±0.001
Spleen	0.109± 0.058	0.028±0.121
Adrenals	0.086± 0.052	0.015±0.001
Lungs	0.006 ±0.001	0.012±0.0004
Urinary bladder wall	0.098± 0.048	0.125±0.062
Red marrow	0.015± 0.003	0.010±0.0004
Total body	0.014± 0.002	0.013±0.0003
Effective dose (mSv/MBq)	0.021±0.003	0.026±0.003

Supplemental Figure 1. Patient with lymph node metastasis from resected ileal NET underwent ^{68}Ga-DOTATATE PET/CT for restaging (*coronal PET, fused PET/CT and PET (A), axial PET, fused PET/CT and CT (C))*. An additional bone metastasis in the right femur was detected resulting in management change (external-beam radiation).

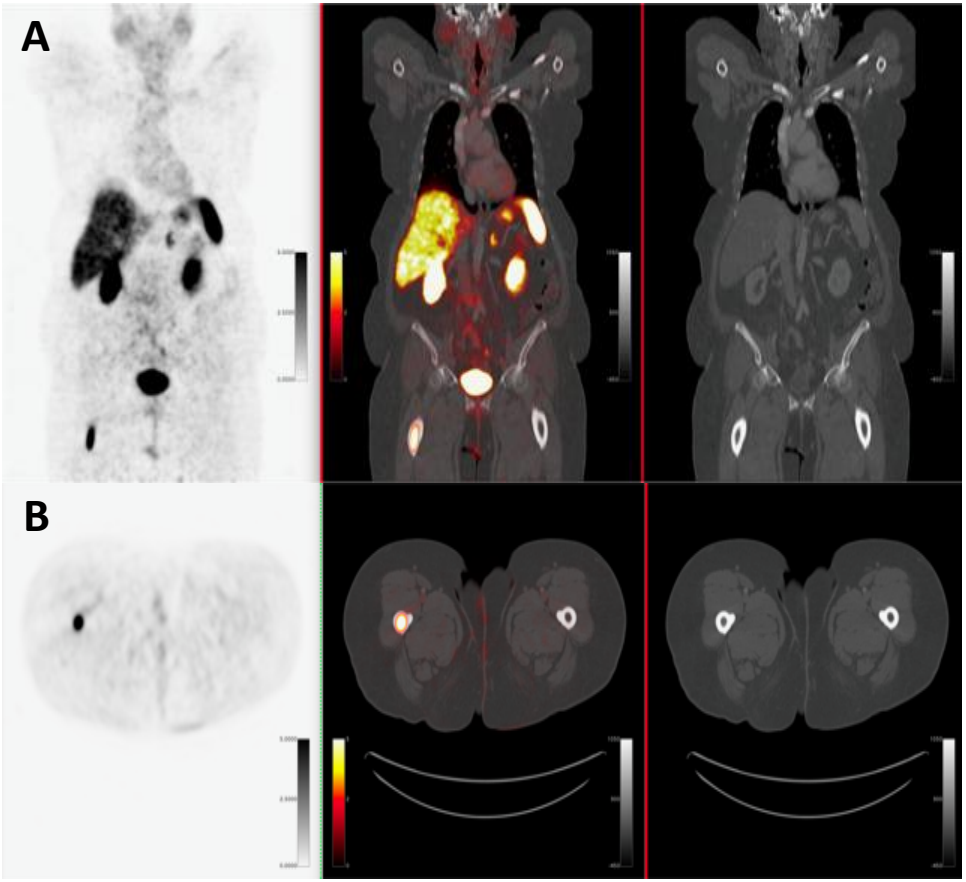

Supplemental Figure 2. A female with a NET underwent a ^{68}Ga-DOTATATE PET/CT to rule out recurrence. The only suspicious finding is evident in the sagittal projections {*PET (A), fused PET/CT (B) and CT (CT)}* exhibiting a clearly intense ^{68}Ga-DOTATATE uptake in the pelvis. Corresponding morphologic information provided by patient history and CT confirmed the presence of a tampon ("hot tampon"); non attenuation corrected images also exhibited increased uptake.

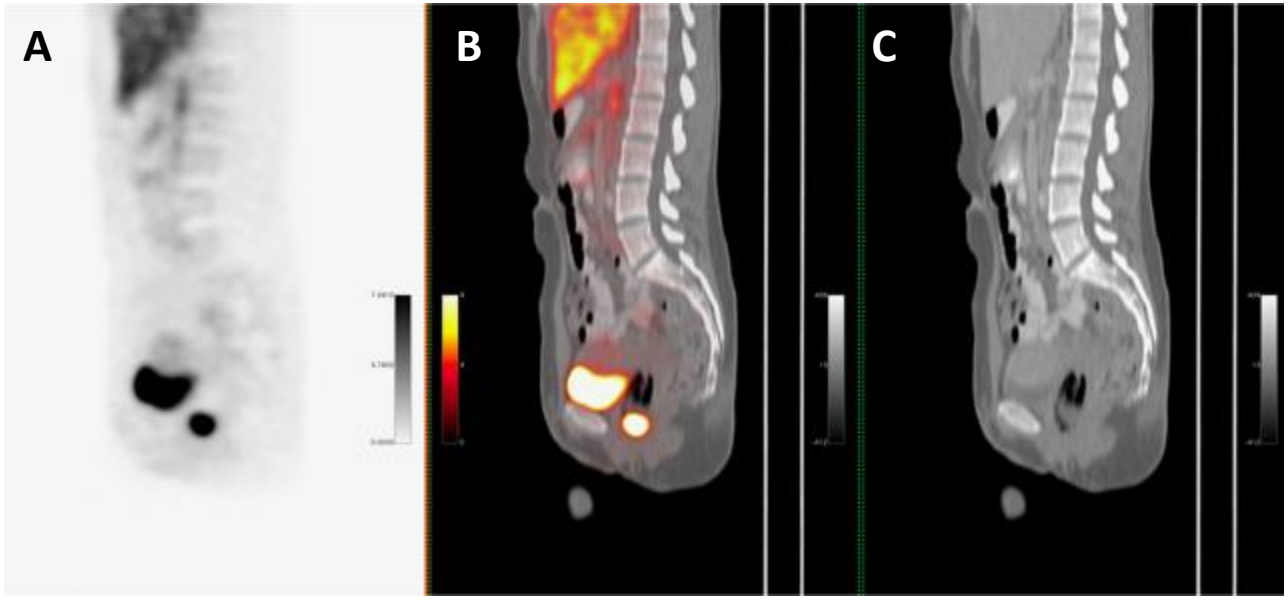

Supplemental Figure 3. Follow-up imaging of a G2 neuroendocrine tumor of the ileocecal valve, status post ileocolic and mesenteric node resection. MRI (C, axial DWI B500 sequence, solid arrow) shows restricted diffusion in subcentimeter foci scattered throughout the liver suspicious for metastases, probably below PET resolution for ^{68}Ga-DOTATATE, which is negative a these sites (B) and only demonstrates a larger lesion in segment 6 (A, solid arrow). ^{68}Ga-DOTATATE, however, demonstrates uptake in borderline enlarged mesenteric nodes (D, E, dashed arrow and circle) adjacent to the surgical clips, peritoneal implants and left breast nodule (A, dotted arrow and arrowhead), which are then characterized as suspicious for recurrence.

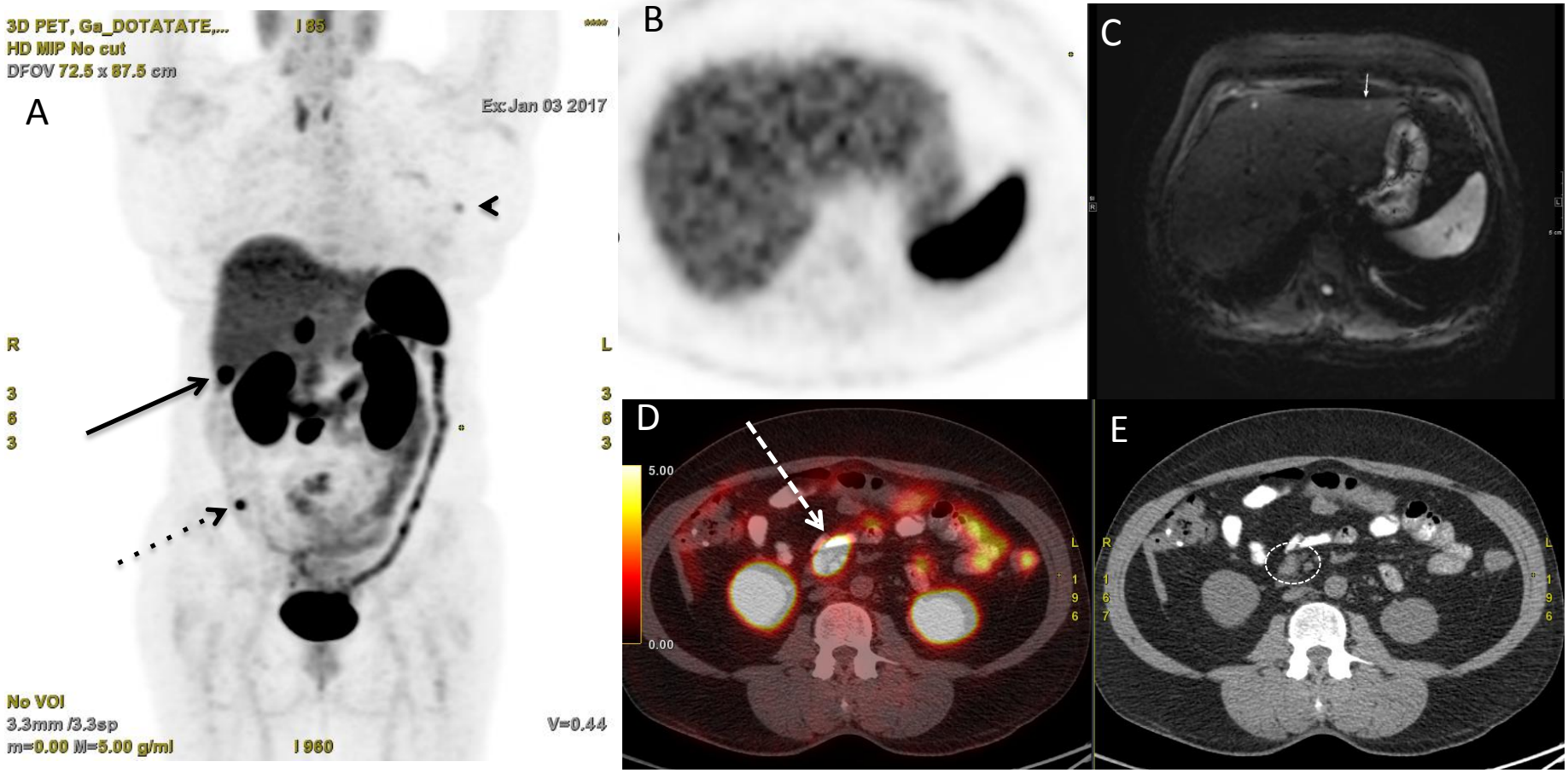

Supplemental Figure 4. Patient affected by an atypical bronchial carcinoid, stage IIIa, status post resection and adjuvant chemotherapy, presenting now with evidence of right hilar node recurrence (A, B, dashed arrow) to guide a possible loco-regional approach. ^{68}Ga-DOTATATE PET/CT revealed the presence of an additional focus of tracer avidity in the left sacrum (C, solid arrow) without CT correlate, however, suspicious for metastasis. A subsequent biopsy confirmed the metastatic etiology. The patient was scheduled for systemic therapy.